Synthesis of matrix-type NiO–SDC composite particles by spray pyrolysis with acid addition for development of SOFC cermet anode

Mitsunobu Kawano [a,*], Hiroyuki Yoshida [a], Koji Hashino [a], Hiroshi Ijichi [b], Seiichi Suda [c], Koichi Kawahara [c], Toru Inagaki [a]

[a] *Energy Use R&D Center, The Kansai Electric Power Co., Inc., 11-20 Nakoji 3-chome, Amagasaki, Hyogo 661-0974, Japan*
[b] *Kanden Power-tech Co. Ltd., 2-1-1800 Benten 1-chome, Minato-ku, Osaka 552-0007, Japan*
[c] *Japan Fine Ceramics Center, 4-1 Mutsuno 2-chome, Atsuta-ku, Nagoya, Aichi 456-8587, Japan*

Abstract

Matrix-type NiO–SDC composite particles were synthesized by spray pyrolysis from the starting solution containing citric acid without pre-heat treatment. Matrix-type composite particles synthesized in this study were spherical shape with high-dispersed state of NiO and SDC. The calcined matrix-type NiO–SDC composite particles at 500 and 1000 °C showed the high performance of SOFC anode. From the electrochemical characterization, the matrix-type structure was effective to reduce the ohmic loss, and the calcination treatment for the matrix-type composite particles would reduce the anodic polarization. It was found that the addition of citric acid into the starting solution for spray pyrolysis led to the high-dispersed matrix-type NiO–SDC composite particles with spherical shape, which showed the high performance anode, without any pre-heat treatment of the starting solution.
© 2007 Elsevier B.V. All rights reserved.

Keywords: Solid oxide fuel cell; Intermediate temperature; Anode; Spray pyrolysis; Composite particles; Citric acid

1. Introduction

Solid oxide fuel cells (SOFCs) are one of the promising power generation systems because they can generate electric power at high-energy conversion efficiency using various fuels. Intermediate temperature SOFCs operating at 600–800 °C have been investigated extensively in recent years because reducing operating temperatures of SOFCs would make it possible to use inexpensive metals for the construction of SOFC system and reduce thermal degradation of SOFCs.

Reducing the operation temperature increases not only the ohmic loss at the electrolyte but also the polarizations at the anode and cathode. Thus, it is of great importance to develop highly active anode with sufficient low polarizations at intermediate temperatures. To develop highly active anodes, long three-phase boundaries (TPBs) are required for anode structures [1]. To lengthen TPBs, SOFC anodes consist of an electronic conductor such as a metal component and an oxide ion conductor. Nickel (Ni) is generally used as a metal component because of its high electronic conductivity, high hydrogen oxidation activity and excellent cost performance. Samaria-doped ceria (SDC) is also one of the desirable materials as an oxide ion conductor in SOFC anode because SDC has the highest ionic conductivity in cation-doped ceria [2–4]. SDC would exert electrochemical activities because SDC also has electronic conductivity. Therefore, the cermet anode of Ni and SDC would be one of the most promising candidates as SOFC anode [5].

To use Ni and SDC as anode materials, there are some drawbacks due to mismatches of thermal expansion and cohesion. Ni tends to sinter easily at relatively low temperatures. Thus, the sintering of Ni will cut off the electrical or oxide ion conduction network structure within Ni–SDC anode. Ni also tends to react with some electrolytes and form the high resistive phase [6].

To resolve these problems, we have investigated NiO–SDC composite particles as a precursor of SOFC anodes [7–13]. NiO–SDC composite particles were synthesized by spray pyrolysis. Comparing with the preparation by solid-state reaction, spray pyrolysis process would have some advantages: (1) small
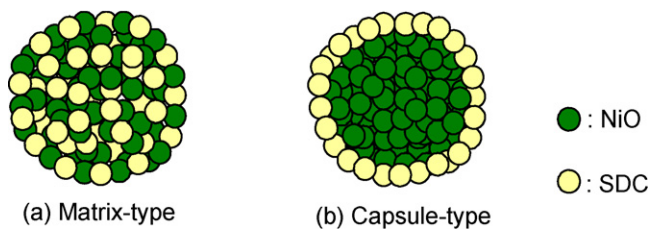

Fig. 1. Schematic illustration of the microstructure of (a) matrix-type and (b) capsule-type NiO–SDC composite particles.

particle size distribution; (2) controllable large particle size ranges from 0.1 to 100 μm; (3) high purity and ease control of composition or morphology [14].

NiO–SDC composite particles we have developed so far have a capsule-type morphology that had NiO covered with SDC [7–11]. The SOFC anode composed of capsule-type NiO–SDC composite particles suppressed the aggregation of Ni and showed the low anodic polarization [7]. The SDC shells need relatively high sintering temperature than the NiO cores, and the SDC shells would suppress Ni aggregation.

However, capsule-type composite particles do not provide a large contact area between Ni and SDC. As compared with capsule-type composite particles, matrix-type composite particles are expected to have a large contact area between Ni and SDC because they are composed of high-dispersed state of Ni and SDC. In Fig. 1, we draw morphological images of (a) matrix-type and (b) capsule-type NiO–SDC composite particles. SOFC anodes derived from the matrix-type composite particles can improve the anodic properties in comparison with capsule-type ones.

Thus, we have synthesized matrix-type NiO–SDC composite particles by spray pyrolysis using the starting solution with ethylene glycol as a chelating reagent and nitric acid [12,13]. In this case, the particles synthesized from the heat-treated starting solution were matrix-type with spherical shape. It was easy to treat and control spherical shape particles, resulted in a high and reproducible anode performance [12]. However, flake-state powders with matrix-type were obtained from the non-heat-treated starting solution. It was difficult to control morphologies of these flake-state powders, resulted in the difficulty with the reproducibility of their anode performance [12].

On the other hand, we have also studied the synthetic conditions of spray pyrolysis by acids addition to the starting solution [11]. Under the consideration of acids addition, citric acid, which is usually used as a chelating reagent [15,16], is considered to be a possible additive for synthesizing matrix-type composite particles, because citric acid has excellent chelating ability without the oxidation by heat treatment to the starting solution. Thus, the particles synthesized from the starting solution with the addition of citric acid are expected to be more dispersive state of Ni and SDC than the particles synthesized from the starting solution with the addition of ethylene glycol.

In this study, we tried to synthesize matrix-type NiO–SDC composite particles from the starting solution containing citric acid without pre-heat treatment. We also studied the SOFC per-

formance at 750 °C using this matrix-type NiO–SDC composite particles as anode materials.

2. Experimental

2.1. Synthesis of NiO–SDC composite particles by spray pyrolysis

NiO–SDC composite particles were synthesized by spray pyrolysis method (Fig. 2). Aqueous starting solutions containing the desired composition of corresponding cations were prepared by dissolving $Ni(NO_3)_2 \cdot xH_2O$ (98.0%, Wako Pure Chemical Industries Ltd.) (or $Ni(CH_3COO)_2 \cdot xH_2O$ (99.9%, Kojundo Chemical Laboratory Co. Ltd.)), $Ce(NO_3)_3 \cdot xH_2O$ (99.9%, Kojundo Chemical Laboratory Co. Ltd.), $Sm(NO_3)_3 \cdot xH_2O$ (99.9%, Mitsuwa Chemicals Co. Ltd.) with the addition of citric acid or nitric acid. In the case of the addition of citric acid, $Ni(NO_3)_2 \cdot xH_2O$ was used as Ni salt. On the other hand, $Ni(CH_3COO)_2 \cdot xH_2O$ was used as Ni salt in the case of the addition of nitric acid to the starting solution [11]. The desired composition of SDC was determined to be $(CeO_2)_{0.8}(SmO_{1.5})_{0.2}$, which gave the highest ionic conductivity [3]. The starting salts were dissolved to make the solution contain $0.08 \, mol \, l^{-1}$ of Ce^{3+} and $0.02 \, mol \, ml^{-1}$ of Sm^{3+} cations, and Ni^{2+} cation was added to the starting solution to give the volume ratio of 1.5:1 as Ni/SDC. Citric acid or nitric acid was also added to the starting solution. The molar concentration of added citric acid or nitric acid was twice as large as that of Ni^{2+} cation to give the sufficient effect of acid addition.

These solutions were atomized using ultrasonic vibrators with an oscillation frequency of 1.65 MHz in an atomizing vessel. Ultrasonic vibrators increased the temperature of the solutions. Cold water was then circulated around the atomizing vessel to keep the temperature of the solutions low, because atomization at relatively high temperature led to inhomogeneous droplets [9]. The droplets were transported into a reaction furnace using air as a carrier gas at a fixed flow rate of $1 \, dm^3 \, min^{-1}$. The reaction furnace consisted of four independent heating zones, whose temperatures were set at 200, 400, 800, and 1000 °C, respectively. The droplets including Ni^{2+}, Ce^{3+}, and Sm^{3+} cations were dried, decomposed, reacted, and sintered during passing through the reaction furnaces. The NiO–SDC particles were collected using a membrane filter with 0.25 μm pores. We denoted the synthesized NiO–SDC composite particles from the starting solution containing citric acid as CA
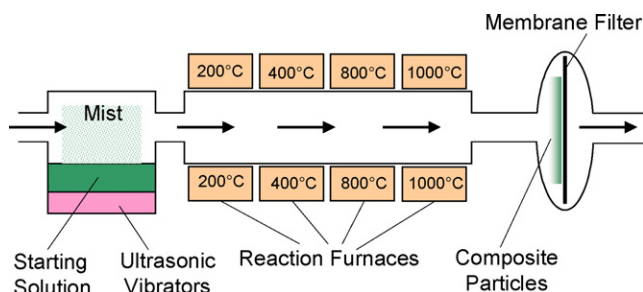

Fig. 2. Schematic illustration of spray pyrolysis.

particles, also denoted the synthesized NiO–SDC composite particles from the starting solution containing nitric acid as NA particles. We also referred to the matrix-type NiO–SDC composite particles synthesized previously by spray pyrolysis using the starting solution with ethylene glycol as a chelating reagent [12,13]. In this paper, we designated the matrix-type particles synthesized from the heat-treated starting solution containing ethylene glycol as EGH particles, and also designated the powders synthesized from the non-heat-treated starting solution containing ethylene glycol as EGN powders. Some of the synthesized particles by spray pyrolysis were calcined at 500 or 1000 °C for 24 h in air.

2.2. Characterizations of NiO–SDC composite particles

X-ray diffraction analysis (XRD, Rigaku RINT-2500) was carried out to confirm that the composite particles possessed the individual NiO and SDC crystal structures. Morphologies of the particles and the anode microstructures were observed by scanning electron microscope (SEM, Hitachi S-2380N or S-4500). The cross section of particles was also observed with a transmission electron microscope (TEM, EM-002B, TOPCON) and EDS (Noran Vantage System) mapping. Samples suitable for TEM observation were prepared by focused ion beam (FIB) or microtomy method.

2.3. Cell fabrication process

Cell fabrication process was reported in detail previously [11]. SOFC single cells were fabricated by applying NiO–SDC composite particles as anode materials, a lanthanum gallate-based substrate which possessed high oxide ionic conductivity [17,18] as an electrolyte, and a samarium cobaltite compound which gave the good performance [19] as a cathode material. For a lanthanum gallate-based electrolyte, we selected the LSGMC of ca. 200 μm in thickness with the chemical formula of $La_{0.8}Sr_{0.2}Ga_{0.8}Mg_{0.15}Co_{0.05}O_{3-\delta}$. For a samarium cobaltite compound, we selected the $Sm_{0.5}Sr_{0.5}CoO_{3-\delta}$ (SSC). For the reference electrode, Pt wire was wound around the LSGMC pellet. Fabricated SOFC single cells had the effective electrode area of 2 cm².

2.4. Single cell performance test

SOFC cell performance tests were carried out at 750 °C. Air was used as an oxidant (ca. 31 ml min⁻¹), and dry hydrogen was used as a fuel (ca. 7.5 ml min⁻¹). NiO in the anode was reduced to Ni under fuel atmosphere prior to the measurement of the power generation characteristics. The current-interruption technique was applied to measure the ohmic loss and the polarization loss at the electrode.

3. Results and discussion

3.1. TEM–EDS maps of NiO–SDC composite particles

We have synthesized two kinds of NiO–SDC composite particles by spray pyrolysis from the starting solutions with citric acid or nitric acid. Ones were the CA particles from the starting solution with citric acid, and the others were NA particles
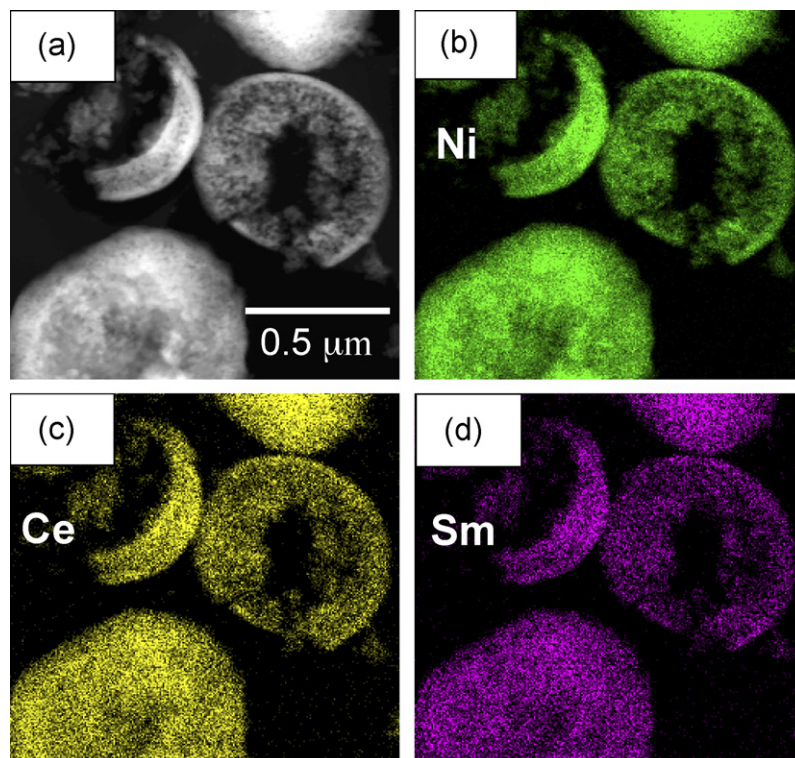

Fig. 3. (a) TEM image of CA particles and the EDS maps of (b) nickel, (c) cerium, and (d) samarium.
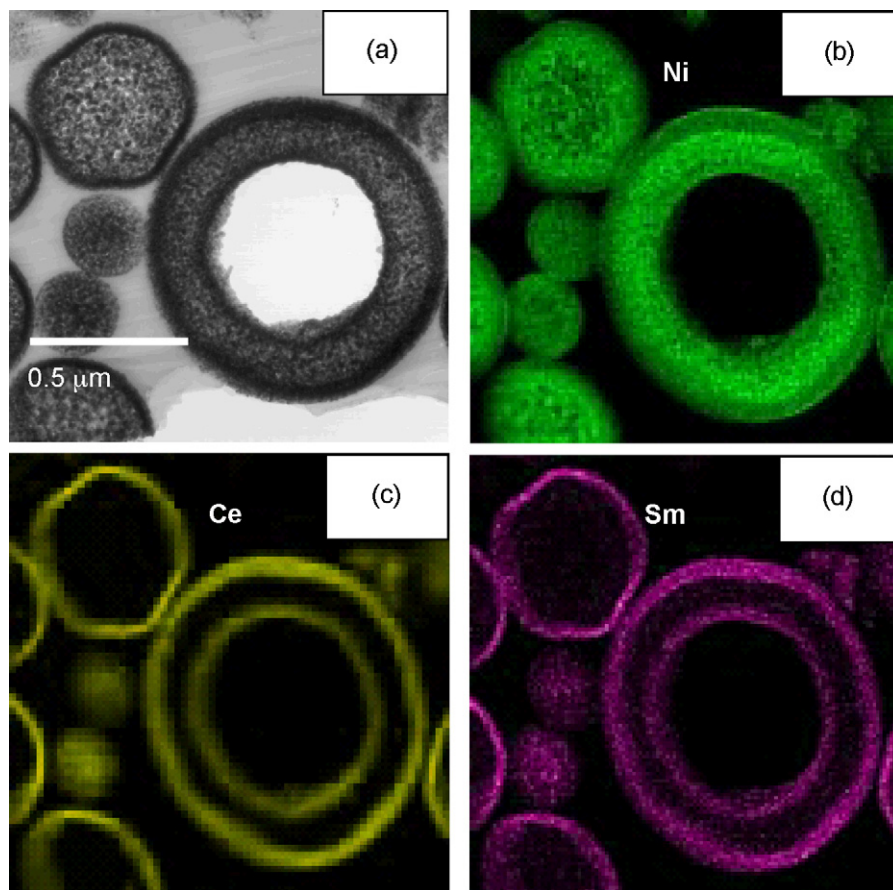
Fig. 4. (a) TEM image of NA particles and the EDS maps of (b) nickel, (c) cerium, and (d) samarium.

from the starting solution with nitric acid. TEM images of CA particles without the calcination and the EDS maps of nickel, cerium, and samarium are shown in Fig. 3, and those of NA particles are also shown in Fig. 4. Fig. 3 reveals that CA particles are spherical shape particles consisted of NiO and SDC, and also reveals that NiO and SDC are dispersed finely in the particles. On the other hand, Fig. 4 indicates that NiO is covered with thin SDC layer in NA particles. Thus, the addition of citric acid into the starting solution resulted in the high-dispersed matrix-type composite particles while the addition of nitric acid did in the capsule-type. We also referred to EGH particles and EGN powders synthesized from the starting solution with ethylene glycol by spray pyrolysis [12,13]. In this case, EGN powders were flake-state under the condition of the non-heat-treated starting solution. It was difficult to control these flake-state powders morphologies, resulted in the difficulty of the reproducibility for their anode performance. EGH particles synthesized from the heat-treated starting solution, however, were matrix-type with spherical shape. It was easy to treat and control spherical shape particles, resulted in a high and reproducible anode performance [12]. Thus, CA particles, which were spherical matrix-type composite particles, were desirable ones similar to EGH particles [12]. The reason of the synthesis of matrix-type composite particles previously reported [12] was the chelating ability of ethylene glycol. In this study, it is

also suggested that the cation (Ni^{2+}, Ce^{3+}, and Sm^{3+}) retained uniform-dispersed state during the synthesis by spray pyrolysis because of the chelation of cations and polymerization in the starting solution containing citric acid [15,16]. Then, the synthesized composite particles consisted of high-dispersed NiO and SDC. We described the schematic illustration of synthesis from the starting solution with citric acid to the composite particles in Fig. 5.
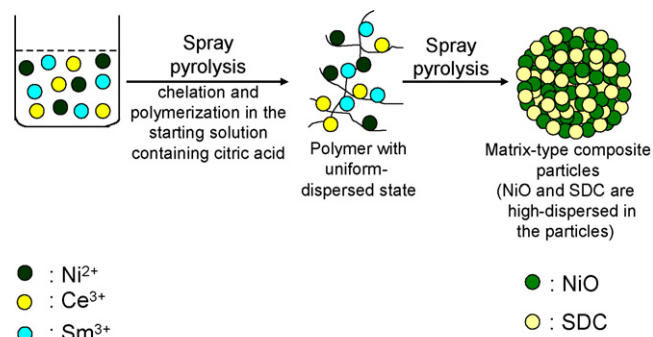

Fig. 5. Schematic illustration of the synthesizing process of matrix-type composite particles during spray pyrolysis from the starting solution with citric acid.
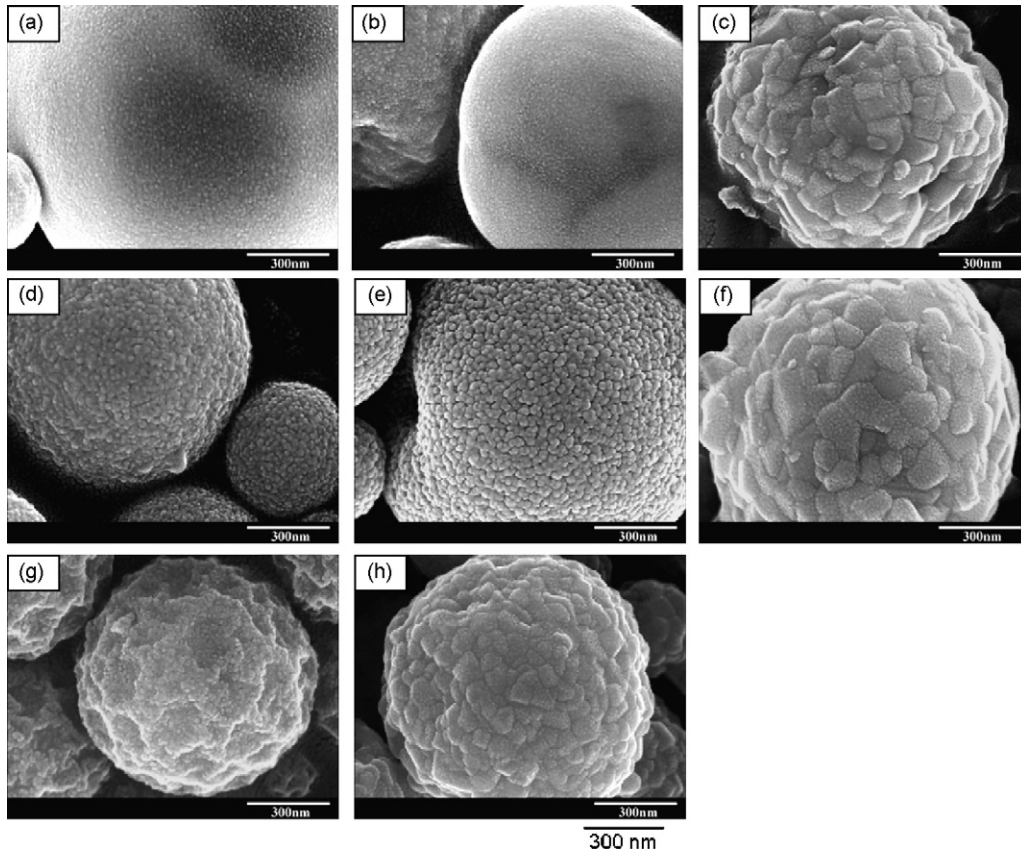
Fig. 6. High magnification of SEM images of matrix-type CA particles (a) as-synthesized and after the calcination at (b) 500 °C and (c) 1000 °C, capsule-type NA particles (d) as-synthesized and after the calcination at (e) 500 °C and (f) 1000 °C, and matrix-type EGH particles (g) as-synthesized and after the calcination at (h) 1000 °C.

3.2. SEM images and X-ray diffraction analysis of NiO–SDC composite particles

High magnification SEM images of CA, NA, and EGH particles either as-synthesized or after the calcinations are shown in Fig. 6. In this paper, we defined that the primary particles were the smallest ones which could be distinguished in these high magnification SEM images. The primary particles of as-synthesized CA in this study (Fig. 6(a)) were fine in comparison with those of NA (Fig. 6(d)). Moreover, the primary particles of as-synthesized CA (Fig. 6(a)) were finer than those of EGH synthesized in previous study (Fig. 6(g)). These results indicate that NiO and SDC in as-synthesized CA particles dispersed more finely than those in NA particles and in EGH particles synthesized in previous study [12,13]. Fig. 6 also shows the effect of the calcination treatment on the primary particles sizes. There were no noticeable difference in the primary particles sizes of as-synthesized (Fig. 6(a): CA; (d): NA) and 500 °C calcined (Fig. 6(b): CA; (e): NA) particles, respectively. On the other hand, the primary particles sizes of 1000 °C calcined particles (Fig. 6(c): CA; (f): NA; (h): EGH) were much larger than those of as-synthesized (Fig. 6(a): CA; (d): NA; (g): EGH) and 500 °C calcined (Fig. 6(b): CA; (e): NA) ones, respectively. These results indicate that the grain growth during the calcination occurred drastically in the temperature range of 500–1000 °C irrespective of the microstructures of the composite particles.

X-ray diffraction analysis was also carried out to examine the individual NiO and SDC crystal structures in NiO–SDC composite particles. Fig. 7 shows the X-ray diffraction patterns of CA particles, which were similar to those of EGH and NA particles. All the peaks detected were ascribed to the NiO and SDC. Thus, there were no by-products in CA, EGH, and NA particles. To investigate these particles morphology more minutely, the crystallite sizes of NiO and SDC concerning about these composite
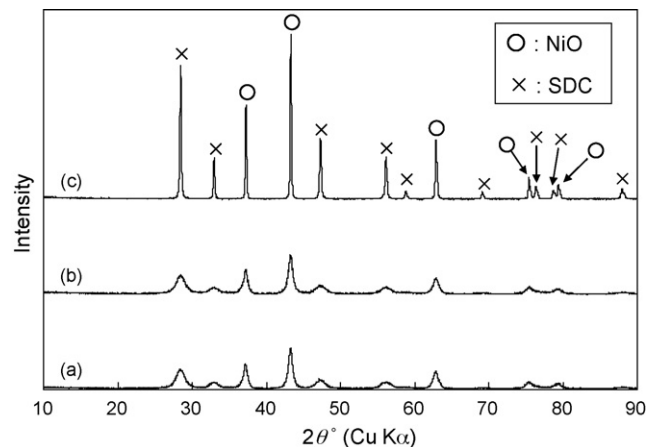

Fig. 7. X-ray diffraction patterns of CA particles (a) as-synthesized and after the calcination at (b) 500 °C and (c) 1000 °C.
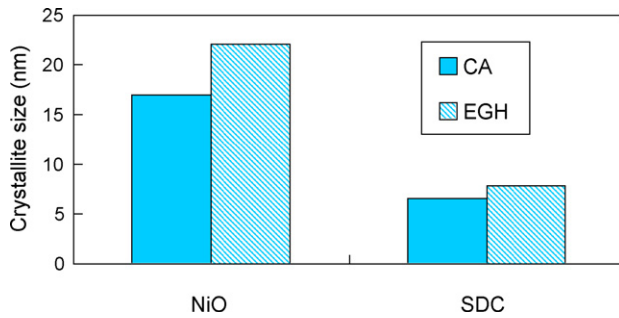
Fig. 8. The crystallite size of CA and EGH matrix-type particles without the calcination treatment.

Fig. 10. Typical *I–V*, *I–P* characteristics of Ni–SDC (CA or NA)/LSGMC/SSC cell at 750 °C using dry hydrogen as a fuel (ca. 7.5 ml min^{-1}).

particles were calculated from the full width at half maximum (FWHM) of X-ray diffraction pattern by using the Scherrer equation. Fig. 8 shows the calculated crystallite sizes of NiO and SDC in both CA and EGH matrix-type as-synthesized composite particles. This figure indicates that crystallite sizes of NiO and SDC in CA particles were smaller than those in EGH particles. Fig. 9 also shows the crystallite sizes of NiO and SDC in both CA and NA particles concerning about the calcination temperature. Both crystallite sizes of NiO and SDC in matrix-type CA particles were smaller than those of NiO and SDC in capsule-type NA particles. Moreover, crystallite sizes of NiO and SDC increased drastically after the calcination at 1000 °C irrespective of the types of composite particles.

These behaviors about the crystallite size derived from the X-ray diffraction analysis had the same tendency as those of the primary particle size derived from SEM images. These results suggest that matrix-type NiO–SDC composite particles did not tend to aggregate compared with capsule-type composite particles and that the grain growth proceeded severely at 500–1000 °C in both matrix-type and capsule-type particles. It is reasonable that matrix-type composite particles did not tend to aggregate because of their fine dispersion compared with capsule-type composite particles. Moreover, from the SEM images (Fig. 6(a) and (g)) and the crystallite sizes (Fig. 8), NiO and SDC in CA particles were more high-dispersed state than those in EGH particles under the comparison of the same as-synthesized matrix-type composite particles (CA and EGH). Thus, these fine dispersions of NiO and SDC in CA particles were expected to improve the performance of anodes which were consisted of them.
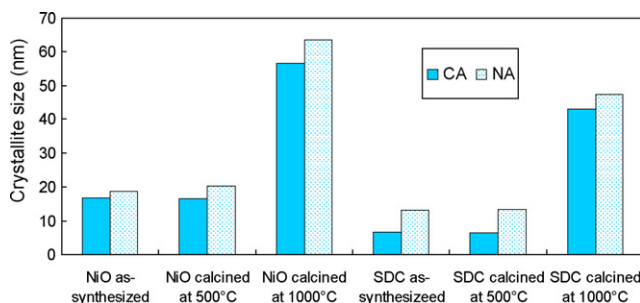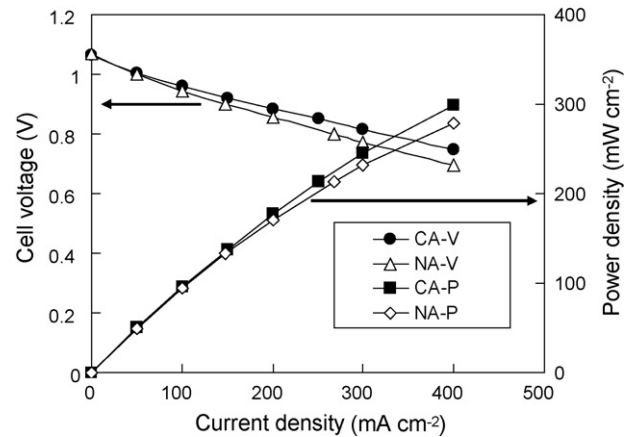
3.3. Single cell performance test

In this section, we compared the SOFC anode performances fabricated from matrix-type CA particles and capsule-type NA particles. Fig. 10 shows the typical *I–V* and *I–P* characteristics of the cells whose anodes were fabricated from matrix-type CA and capsule-type NA particles calcined at 1000 °C for 24 h. These results indicate that the cell performance whose anode was fabricated from CA particles was higher than that whose anode was fabricated from NA particles. It is considered that the dispersion of NiO and SDC in the composite particles was effective for the improvement of SOFC anode. To investigate the relationship between the morphology of matrix-type CA particles and their anode performance in detail, the dependence of calcination temperature for the anode performance was also studied. Three kinds of Ni–SDC anode were fabricated using CA particles, which were as-synthesized and after the calcination at 500 and 1000 °C for 24 h. In comparison, two kinds of Ni–SDC anode were also fabricated using capsule-type NA particles which were as-synthesized and after the calcination at 1000 °C for 24 h. Multiple performance tests were carried out using SOFC cells with anodes made from the same particles to confirm the reproducibility of the cell performance. The average SOFC power densities at 0.3 A cm^{-2} with 750 °C using dry hydrogen (ca. 7.5 ml min^{-1}) as a fuel are shown in Fig. 11(a). In the case of CA particles, the cell performance increased after the calcination treatment at 500 and 1000 °C for the particles. On the other hand, in the case of NA particles, the cell performance deteriorated after the calcination treatment at 1000 °C for the particles. The effect of the calcination on SOFC cell performance was opposite for CA and NA particles. It is considered that these differences would be originated from the difference of the dispersion of NiO and SDC in CA and NA particles. The cell performance, however, whose anodes were fabricated from CA particles with the calcination treatment were somewhat higher than that whose anodes were fabricated from NA particles as-synthesized (Fig. 11(a)). Thus, the application of matrix-type NiO–SDC composite particles as anode materials improved the SOFC cell performance.

Fig. 9. The relationship between the crystallite size and the calcination temperature of CA and NA particles.
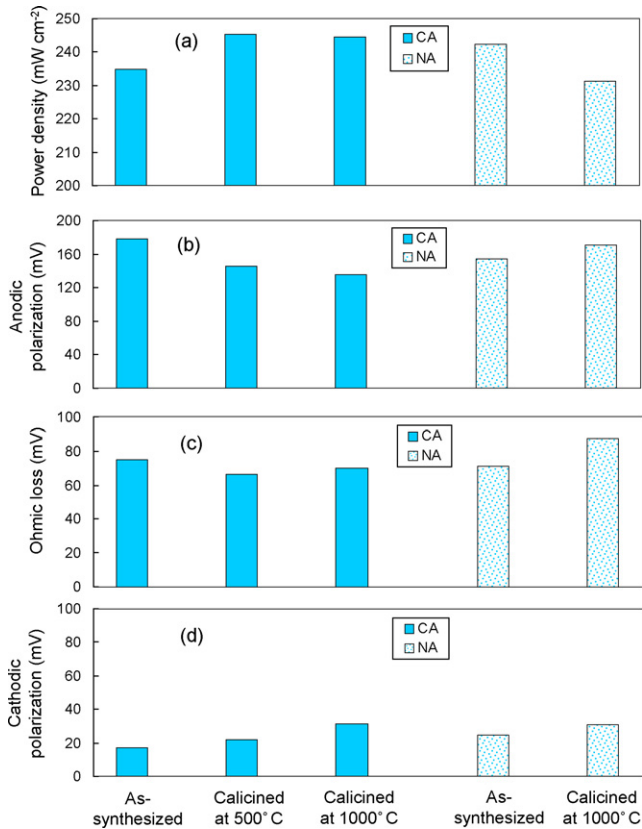
Fig. 11. The average (a) power densities, (b) anodic polarizations, (c) ohmic losses, and (d) cathodic polarizations of various Ni–SDC (CA or NA)/LSGMC/SSC cell at 0.3 A cm^{-2} with 750 °C using dry hydrogen as a fuel (ca. 7.5 ml min^{-1}).

The average voltage losses of SOFC due to the anodic polarization, the ohmic loss and the cathodic polarization obtained by applying CA and NA particles without or with the calcination treatment are shown in Fig. 11(b)–(d), respectively. As shown in Fig. 11(d), the cathodic polarizations were very low values in the range of only ca. 20–30 mV regardless of NiO–SDC anode

materials. These results indicate that SSC applied for the cathode material in this study gave high performance such as reported in Ref. [19]. While the average power densities (Fig. 11(a)) and ohmic losses (Fig. 11(c)) for various kinds of cells contained the effect of the cathodic reaction, it is considered that the influence of the cathodic resistance used in this study was very small and negligible because of the low and constant resistance of the cathode as shown in Fig. 11(d). In addition, cathode (SSC) and electrolyte (LSGMC) were fixed in this study while various kinds of NiO–SDC anode materials (matrix-type CA or capsule-type NA, with or without the calcination treatment) were used. Then, it is considered that the effects of the cathode and the electrolyte were almost constant for the cell performance. Using matrix-type CA particles as anode materials, the calcination treatment had the effect of the decrease in the anodic polarization (Fig. 11(b)). On the other hand, in the case of capsule-type NA particles, the anodic polarizations became larger by applying the particles calcined at 1000 °C (Fig. 11(b)). These contrastive effects of the calcination on the anodic polarization indicate that there would be a suitable dispersion of NiO and SDC in the particles which will determine the suitably connected network structure of Ni and SDC and TPB area as the anode. In Fig. 11(c), the average ohmic losses of the cell using matrix-type CA particles showed that the calcination treatment made no differences and they were lower than those using capsule-type NA particles. These results suggest that matrix-type structures are effective to reduce the ohmic loss probably because SDC did not retard Ni network structure. This effect of reducing the ohmic loss using matrix-type composite particles as anode materials was previously reported [12,13]. Thus, it is considered that the reduction of the ohmic loss is the nature of matrix-type composite particles.

SEM images of anode surface fabricated from CA particles after the SOFC power generation are shown in Fig. 12(a)–(c). In the case of applying CA particles, the anodes fabricated from the particles calcined at 500 and 1000 °C (Fig. 12(b) and (c)) looked having the thick network structure compared with the
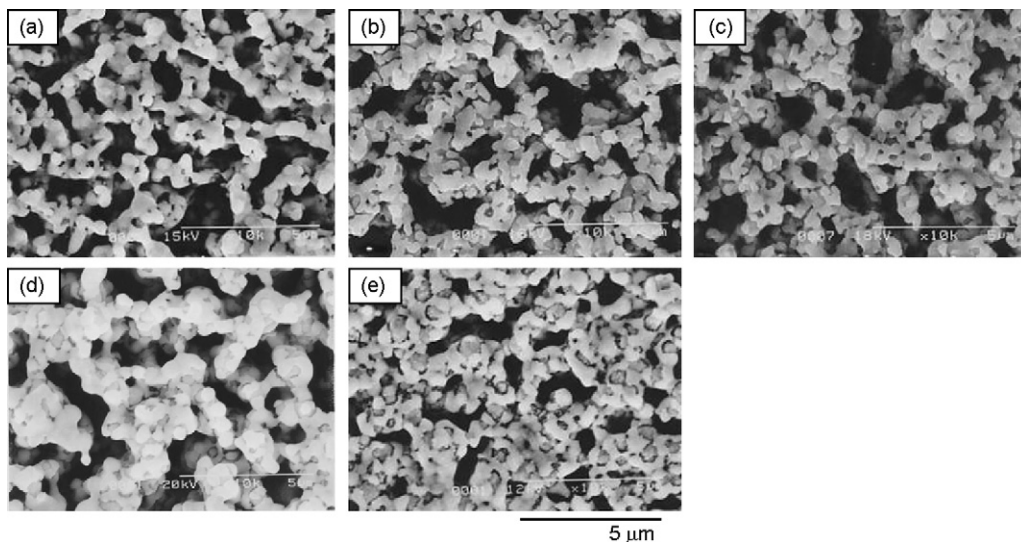

Fig. 12. SEM images of the anode surface after the power generation fabricated from matrix-type CA particles (a) as-synthesized and calcined at (b) 500 °C and (c) 1000 °C, and capsule-type NA particles (d) as-synthesized and calcined at (e) 1000 °C.

anode fabricated from the particles without the calcination treatment (Fig. 12(a)). Fig. 12(a)–(c) indicates that the dispersions of NiO and SDC in the CA particles depends on the calcination conditions and determined the evolution of anode network structure. Therefore, the anodes fabricated from CA particles calcined at 500 and 1000 °C would show low anodic polarizations (Fig. 11(b)) probably because they had the suitably connected network structure and large TPB area. However, the ohmic losses of the cell using CA particles as anode materials (Fig. 11(c)) were almost low and constant with or without the calcination treatment. Then, to clarify the behavior of ohmic losses, we measured the conductivity of LSGMC electrolyte used in this study by DC four probes method. The measured conductivity of LSGMC was 0.105 S cm^{-1} at 750 °C which was same as the operation temperature of SOFC cell demonstrated in this study. Considering that the thickness of LSGMC electrolyte used in this study was ca. 200 μm, the ohmic loss due to the LSGMC electrolyte was calculated as ca. 57 mV at 0.3 A cm^{-2} with 750 °C. As described in Fig. 11(c), the ohmic losses of overall cells whose anodes were fabricated from CA particles were in the range of ca. 65–75 mV at 0.3 A cm^{-2} with 750 °C. Then, it is considered that the influence of the calcination treatment for the ohmic losses of overall cells became obscure because the ohmic loss due to the LSGMC electrolyte (ca. 57 mV) was the major part of the ohmic losses of overall cells whose anodes were fabricated from CA particles (ca. 65–75 mV). Moreover, as mentioned above, the reduction of the ohmic loss is the nature for matrix-type composite particles [12,13]. Then, it is considered that lower ohmic losses fabricated from matrix-type CA particles (ca. 65–75 mV) than those fabricated from capsule-type NA particles (ca. 75–90 mV) as shown in Fig. 11(c) should cause the difficulty to discriminate the influence of the calcination treatment for the anode materials. Then, it is concluded that the effect of the calcination treatment to CA particles for the ohmic losses (Fig. 11(c)) was obscure because of the major part of ohmic losses due to the LSGMC electrolyte. However, it is also concluded that reducing ohmic loss was the nature of matrix-type CA particles in comparison with the capsule-type NA particles (Fig. 11(c)) as reported in Refs. [12,13].

From the data of the electrochemical characterization (Fig. 11) and SEM images (Fig. 12), the anodes fabricated from matrix-type CA particles calcined at 500 and 1000 °C showed higher performance among the composite particles used in this study. The improved anode performance would be ascribed to the large contact area of Ni and SDC. Matrix-type CA particles were, then, effective as precursors of the high performance SOFC anode. However, the relationship between the morphology of NiO–SDC composite particles synthesized by spray pyrolysis and their anode structures after the firing at 1280 °C and reduction treatment was still vague. As we reported in Ref. [7], Ni–SDC anode gave very low anodic polarization because aggregation of Ni could be prevented by the presence of SDC between particles at the early stage of sintering in the case of capsule-type NA particles. In the case of matrix-type CA particles, the same effect as capsule-type NA particles and the other effect as providing large contact area are considered but are not defined at present. Thus, we are currently investigating and will report the relationship between the morphology of matrix-type CA particles and their anode structures.

4. Conclusions

Matrix-type NiO–SDC composite CA particles with spherical shape could be synthesized from the starting solution containing citric acid without pre-heat treatment. It was found that the chelation of cations and polymerization in the starting solution containing citric acid resulted in matrix-type CA particles with high-dispersed state of NiO and SDC. Matrix-type CA particles calcined at 500 and 1000 °C showed high performance. It is considered that the matrix-type structure was effective to reduce the ohmic loss probably because SDC did not retard Ni network structure in the anode fabricated from matrix-type composite particles. It is also considered that the calcination treatment at 500 and 1000 °C for the matrix-type composite particles would reduce the anodic polarization probably because of the suitably connected network structure of Ni and SDC and large TPB area. It is concluded that matrix-type NiO–SDC composite particles synthesized from the starting solution containing citric acid by spray pyrolysis were effective for the improvement of SOFC anode performance.

References

[1] A. Atkinson, S. Barnett, R.J. Gorte, J.T.S. Irvine, A.J. Mcevoy, M. Mogensen, S.C. Sighal, J. Vohs, Nat. Mater. 3 (2004) 17.
[2] K. Eguchi, T. Setoguchi, T. Inoue, H. Arai, Solid State Ionics 52 (1992) 165.
[3] H. Yahiro, Y. Eguchi, K. Eguchi, H. Arai, J. Appl. Electrochem. 18 (1988) 527.
[4] S. Zhao, R.J. Gorte, Appl. Catal. A: Gen. 277 (2004) 129.
[5] T. Misono, K. Murata, T. Fukui, J. Chaichanawong, K. Sato, H. Abe, M. Naito, J. Power Sources 157 (2006) 754.
[6] K. Huang, R. Tichy, J.B. Goodenough, C. Milliken, J. Am. Ceram. Soc. 81 (1998) 2581.
[7] H. Yoshida, T. Inagaki, K. Hashino, M. Kawano, S. Takahashi, S. Suda, K. Kawahara, in: S.C. Singhal, J. Mizusaki (Eds.), Proceedings of the Solid Oxide Fuel Cells IX. The Electrochemical Society Proceedings Series (PV2005-07), Pennington, NJ, 2005, p. 1382.
[8] S. Suda, M. Itagaki, E. Node, S. Takahashi, M. Kawano, H. Yoshida, T. Inagaki, J. Eur. Ceram. Soc. 26 (2006) 593.
[9] S. Suda, S. Takahashi, M. Kawano, H. Yoshida, T. Inagaki, Solid State Ionics 177 (2006) 1219.
[10] H. Yoshida, H. Deguchi, M. Kawano, K. Hashino, T. Inagaki, H. Ijichi, M. Horiuchi, K. Kawahara, S. Suda, Solid State Ionics 178 (2007) 399.
[11] M. Kawano, H. Yoshida, K. Hashino, H. Ijichi, S. Suda, K. Kawahara, T. Inagaki, Solid State Ionics 177 (2006) 3315.
[12] S. Suda, K. Kawahara, M. Kawano, H. Yoshida, T. Inagaki, J. Am. Ceram. Soc. 90 (2007) 1094.
[13] K. Kawahara, S. Suda, S. Takahashi, M. Kawano, H. Yoshida, T. Inagaki, Proceedings of the 30th International Conference on Advanced Ceramics and Composites, Cocoa-beach, USA, 2006, CD-Rom.
[14] G.L. Messing, S.C. Zhang, G.V. Javanthi, J. Am. Ceram. Soc. 76 (1993) 2707.
[15] E.E. Boakye, P. Mogilevsky, J. Am. Ceram. Soc. 88 (2005) 2740.
[16] E. Gidarakos, A. Giannis, Water Air Soil Pollut. 172 (2006) 295.
[17] T. Ishihara, H. Matsuda, Y. Takita, J. Am. Chem. Soc. 116 (1994) 3801.
[18] T. Ishihara, T. Akbay, H. Furutani, Y. Takita, Solid State Ionics 113–115 (1998) 585.
[19] T. Ishihara, M. Honda, T. Shibayama, H. Minami, H. Nishiguchi, Y. Takita, J. Electrochem. Soc. 145 (1998) 3177.